

Bound magnetic polaron hopping and giant magnetoresistance in magnetic semiconductors and nanostructures

A. G. Petukhov and M. Foygel

Department of Physics, South Dakota School of Mines and Technology, Rapid City, South Dakota 57701

(Received 19 January 1999; revised manuscript received 5 May 1999)

A theory of bound magnetic polaron (BMP) hopping, driven by thermodynamic fluctuations of the local magnetization, has been developed. It is based on a two-site model of the BMP. The BMP hopping probability rate was calculated in the framework of the ‘‘golden rule’’ approach by using the Ginzburg-Landau effective Hamiltonian method. The theory explains the main features of the hopping resistivity observed in a variety of experiments in dilute magnetic semiconductors and magnetic nanocomposites, namely, (a) the negative giant magnetoresistance, the scale of which is governed by a magnetic polaron localization volume, and (b) the low-magnetic-field positive magnetoresistance which usually precedes the negative magnetoresistance. It is shown that the positive magnetoresistance is a signature of the fluctuation-driven bound magnetic polaron hopping. This effect is related to the vector nature of the magnetic order parameter affected by the presence of the localized-electron spin.

I. INTRODUCTION

Spin-polarized electronic transport in solids has attracted much interest mainly due to discovery of giant magnetoresistance (GMR) and the development of new device applications (high-speed magnetic sensors and memory elements) based on this phenomenon.¹ Several different mechanisms have been proposed for the spin-dependent GMR. Their common feature is the exchange interaction of charge carriers with the itinerant and/or localized magnetic moments of transition- or rare-earth-metal atoms.

Three types of mechanisms can be responsible for the spin-dependent GMR in nonsuperconducting magnetic structures: (1) noncoherent transport of carriers in extended energy-band states across metal magnetic multilayers,^{2,3} (2) tunneling through a junction of two magnetic electrodes separated by an insulating layer,^{4,5} and (3) electron hopping in a system in which a carrier strongly interacts with the localized magnetic moments of either transition-metal atoms (e.g., in dilute magnetic semiconductors⁶) or of rare-earth atoms (e.g., in ErAs/GaAs nanostructures.⁷) In this paper, we will restrict ourselves to case (3), the hopping conductivity in magnetic semiconductors and nanostructures. In these systems, an electron or hole trapped by any kind of attractive potential of a defect, quantum dot, etc., can form a ‘‘cloud’’ of aligned spins of the surrounding magnetic atoms. The creation of such a complex [referred to as a bound magnetic polaron (BMP) (Refs. 8 and 9)] will further lower the free energy of the system by a quantity W_p called a polaron shift. A consistent semiclassical analysis of BMP formation in dilute magnetic semiconductors was given by Dietl and Spálek,¹⁰ while its quantum-mechanical generalization was developed by Wolff *et al.* (for references see Ref. 11). This theory successfully described the spin-flip Raman scattering in magnetic semiconductors.⁶

In order to describe the BMP hopping conductivity, we need, first, to specify the mechanism of an elementary hopping event. Dietl *et al.*^{6,12} considered a ‘‘static’’ picture in

which the electron is transferred from an occupied site to an empty one with frozen equilibrium local magnetizations at both sites. For two identical sites this process is driven by absorption of an acoustic phonon and requires an activation energy of $2W_p$.^{12,13} Another mechanism takes into account thermodynamic fluctuations of the local magnetizations that control the elementary hopping act.^{13,14} Indeed, since the electron energy levels at both sites follow the fluctuations of local magnetic order parameters, it is likely that the levels at the occupied and empty sites will move in opposite directions, thus getting into resonance. For this to occur, the occupied site should spontaneously decrease its local magnetization while the empty one should increase it. The electron can then tunnel from one site to another resonantly. This process somewhat resembles the multiphonon mechanism of small-polaron hopping.^{15,16} It requires an activation energy $W_p/2$ (Ref. 13) which is 4 times smaller compared to that of the ‘‘static’’ mechanism.

The giant negative magnetoresistance observed in dilute magnetic semiconductors was properly attributed by many authors^{6,8} to the BMP phenomenon. Indeed, the application of a large magnetic field will quench magnetic polarons by reducing the magnetic part of their binding energy and therefore the activation energy of the hopping conductivity. However, the presence of a significant (up to 300%) positive magnetoresistance, which is typical for situations when the carriers are localized,⁶ remains unclear. We will show that the latter is a signature of the fluctuation BMP hopping mechanism and ultimately reflects the fact that, in contrast to conventional lattice polarons, the BMPs are described by a vector order parameter. We will develop a unified and consistent semiclassical description of BMP hopping based on the Ginzburg-Landau effective Hamiltonian formalism^{10,17} and Holstein’s occurrence probability approach.¹⁵ It will be shown that the fluctuation-driven BMP hopping may lead to a nonmonotonic behavior of magnetoresistance. (Recently, a simple two-site model of this kind has been applied to a description of the resistance, including the GMR, of the ErAs islands in GaAs.¹⁸) Our approach also allows us to take into

account a single-phonon-assisted BMP hopping of the Miller-Abrahams type.¹⁹ This process plays a dominant role at high magnetic fields when the polaron shift W_p is small compared to the typical scatter of the nonmagnetic parts of the electron energy levels.

The paper is organized in the following way. In Sec. II, a two-site model of the BMP hopping will be considered. In Sec. III it will be applied to the calculation of the BMP hopping rate. The BMP hopping conductivity and magnetoresistance are calculated in Secs. IV and V. Section VI contains a comparison of our results with experimental data on GMR in magnetic semiconductors and nanocomposites.

II. TWO-SITE MODEL OF THE BMP

Let us consider two centers, 1 and 2, separated by a distance r_{12} . We assume that each site can localize an electron even when no magnetic forces are involved. In the vicinity of each center there is a finite concentration of localized magnetic moments that is described by the spatial distribution of the local magnetization vectors $\vec{M}_{1,2}(\vec{r})$ generated by a fluctuating field of atomic spins. The effective Hamiltonian of the problem is

$$H = H_1 + H_2 + H_{12} + H_{e-ph}, \quad (1)$$

where

$$H_l = \epsilon_l n_l - \frac{1}{2} \hat{\sigma}_l \vec{\Delta}_l + \frac{1}{2\chi} \int \delta \vec{M}_l^2(\vec{r}) d\vec{r} \quad (2)$$

is the Hamiltonian of a bound magnetic polaron localized at a site l ($l=1,2$). Here $n_l = \sum_{\sigma=\pm 1} a_{l\sigma}^\dagger a_{l\sigma}$ is an occupation number of site l (there is only one electron per two sites, i.e., $n_1 + n_2 = 1$); ϵ_l is the ‘‘bare’’ energy of a bound electron at the site l . The second term in Eq. (2) describes the exchange interaction between the trapped electron and localized atomic spins of the magnetic atoms within the region of electron localization together with the direct interaction with the magnetic field \vec{B} taken into account, where

$$\vec{\Delta}_l = \frac{\Gamma_{ex}}{g\mu_B} \int |\Psi_l(\vec{r})|^2 \vec{M}_l(\vec{r}) d\vec{r} + g^* \mu_B \vec{B} \quad (3)$$

is a vector of the local-exchange field, the magnitude Δ_l of which is equal to the Zeeman splitting of the local electron state with the wave function Ψ_l . The vector $\vec{\Delta}$, as a rule, is not directed along the local average magnetic field inside the localization region. Here Γ_{ex} is an exchange coupling constant, μ_B is Bohr’s magneton, g and g^* are the Lande factors of the atomic spin and that of a free electron, and $\hat{\sigma}_l = (\hat{\sigma}_l^x, \hat{\sigma}_l^y, \hat{\sigma}_l^z)$ with $\hat{\sigma}_l^\alpha$ being the conventional Pauli matrices. The last term in Eq. (2) represents the lowest term in the Ginzburg-Landau expansion^{10,17} of the free energy of atomic spins. With \vec{M}_0 being the equilibrium magnetization vector,

$$\delta \vec{M}_l^2(\vec{r}) \equiv [\vec{M}_l(\vec{r}) - \vec{M}_0]^2 \quad (4)$$

is a squared fluctuation of magnetization at the site l . We assume that our medium is described by means of a macroscopic, scalar, and isotropic magnetic susceptibility $\chi(B, T)$. In the effective Hamiltonian (1), the term

$$H_{12} = -t(r_{12}) \sum_{\sigma=\pm 1} (a_{1\sigma}^\dagger a_{2\sigma} + \text{c.c.}) \quad (5)$$

is responsible for electronic hopping between the sites 1 and 2. As a starting point, we assume that spin-flip processes are forbidden. Due to an exponentially small hopping integral

$$t = t(r_{12}) = t_0 \exp(-r_{12}/a), \quad (6)$$

where a is a localization radius of the electron at any of two centers, we will treat H_{12} as a small perturbation. In Eqs. (5) and (2), the operator $a_{l\sigma}^\dagger$ ($a_{l\sigma}$) describes creation (annihilation) of an electron at the site l with spin parallel ($\sigma=1$) or antiparallel ($\sigma=-1$) to the external magnetic field \vec{B} .

It is important to note that in the case of large semiclassical atomic spins, as shown by Wolff and co-workers,¹¹ the effective Hamiltonian (2) is equivalent to the standard s - d model given the fluctuations are Gaussian. (See also Appendix A.) For this effective Hamiltonian we chose the z -axis direction to be along the external field \vec{B} . However, in this representation the local Hamiltonians H_1 and H_2 are not diagonal with respect to the electronic spin quantum numbers. It is convenient to make the following spinor unitary transformation to a new representation in which the spin quantization axes are different and taken to be parallel to the local vectors $\vec{\Delta}_l$:

$$\begin{aligned} a_{l\uparrow}^\dagger &= \exp(i\phi_l/2) [\cos(\theta_l/2) b_{l\uparrow}^\dagger - \sin(\theta_l/2) b_{l\downarrow}^\dagger], \\ a_{l\downarrow}^\dagger &= \exp(-i\phi_l/2) [\sin(\theta_l/2) b_{l\uparrow}^\dagger + \cos(\theta_l/2) b_{l\downarrow}^\dagger]. \end{aligned} \quad (7)$$

It gives

$$\begin{aligned} H &= \sum_{l=1,2} \left(\epsilon_l n_l - \frac{1}{2} n_l \hat{\sigma}_l^z \Delta_l + \frac{1}{2\chi} \int \delta \vec{M}_l^2(\vec{r}) d\vec{r} \right) \\ &\quad - \sum_{\sigma_1, \sigma_2=\pm 1} (\bar{t}_{\sigma_1 \sigma_2} b_{1, \sigma_1}^\dagger b_{2, \sigma_2} + \text{c.c.}) + H_{e-ph}, \end{aligned} \quad (8)$$

where b_{l, σ_i}^\dagger (b_{l, σ_i}) is an operator of the creation (annihilation) of an electron at site i with spin parallel (or antiparallel) to the direction of the local exchange field $\vec{\Delta}_i$; the angles θ_l and ϕ_l define the direction of the vector $\vec{\Delta}_l$ in the original coordinate system. In the absence of spin-flip processes, the squared moduli of the modified transfer integral \bar{t} are equal to

$$|\bar{t}_{\sigma_1, \sigma_2}|^2 = |t|^2 [\delta_{\sigma_1, \sigma_2} \cos^2(\theta_{12}/2) + (1 - \delta_{\sigma_1, \sigma_2}) \sin^2(\theta_{12}/2)], \quad (9)$$

where θ_{12} is the angle between the vectors of the local-exchange field $\vec{\Delta}_1$ and $\vec{\Delta}_2$. In Eqs. (1) and (9), the term H_{e-ph} describes the electron-phonon interaction.

III. BMP HOPPING RATE

Let us assume that initially the electron is localized at site $l=1$ while site $l=2$ is empty, i.e., $n_1=1$, $n_2=0$. In the final state, after the hop, $n_1=0$ and $n_2=1$. We treat the last two terms in the modified Hamiltonian (8) as a small perturbation. By applying the ‘‘Fermi golden rule’’^{17,20} with subse-

quent statistical averaging over initial states, one can calculate the BMP hopping rate in the so-called nonadiabatic regime,¹⁵ when the small hopping integral (6) controls the probability of the hopping event:

$$w_{12} = \frac{2\pi}{\hbar Z_i} \sum_{\sigma_1, \sigma_2} \int \int \mathcal{D}\vec{M}_1 \mathcal{D}\vec{M}_2 |\bar{t}_{\sigma_1 \sigma_2}|^2 \times \exp(-E_{i\sigma_1}/T) f(E_{i\sigma_1} - E_{f\sigma_2}), \quad (10)$$

where

$$f(E) = \delta(E) + \sum_q |\Lambda_q|^2 [N_q \delta(E + \hbar\omega_q) + (N_q + 1) \delta(E - \hbar\omega_q)]. \quad (11)$$

Here only single-phonon processes were taken into account.

In Eq. (10), $\mathcal{D}\vec{M}_l$ means functional integration over all possible configurations of the local magnetizations $\vec{M}_l(\vec{r})$. The energies of the initial ($n_1=1, n_2=0$) and final ($n_1=0, n_2=1$) states [see Eq. (2)] are functionals of magnetization:

$$E_{i\sigma_1} = \epsilon_1 - \frac{1}{2} \sigma_1 \Delta_1 + \frac{1}{2\chi} \int [\delta\vec{M}_1^2(\vec{r}) + \delta\vec{M}_2^2(\vec{r})] d\vec{r}, \quad (12a)$$

$$E_{f\sigma_2} = \epsilon_2 - \frac{1}{2} \sigma_2 \Delta_2 + \frac{1}{2\chi} \int [\delta\vec{M}_1^2(\vec{r}) + \delta\vec{M}_2^2(\vec{r})] d\vec{r}, \quad (12b)$$

where $\delta\vec{M}_l^2(\vec{r})$ is given by Eq. (4), and

$$Z_i = \sum_{\sigma=\pm 1} \int \int \mathcal{D}\vec{M}_1 \mathcal{D}\vec{M}_2 \exp\left(-\frac{E_{i\sigma}}{T}\right) \quad (13)$$

is the partition function of the initial state. In Eq. (11) the δ functions describe energy conservation during the tunneling process without and with absorption or emission of acoustical phonons, the combined index q represents both the wave vector and the branch number of a phonon with the energy $\hbar\omega_q$, and N_q is Planck's distribution function. The matrix element of electron-phonon coupling Λ_q is given in Appendix B.

The expression (10) is derived under the assumptions that (a) the spin of the electron follows an instantaneous configuration of the local atomic spins at the site where it is localized and (b) the electron hopping integral $|t| \ll (W_p T)^{1/2}$. The last assumption is well known in the theory of small lattice polarons as the nonadiabatic hopping regime.¹⁵ Taking $W_p = 10\text{--}100$ K, $|t_0| = 0.1\text{--}1$ eV, and $T = 1$ K, one can find that this assumption is valid if the typical hopping range \bar{r} exceeds several (five to eight) localization radii a , which is definitely true for ErAs/GaAs nanostructures and lightly doped dilute magnetic semiconductors (DMSs). For instance, if $a \approx 10$ Å, the condition $\bar{r}/a > 8$ means that the impurity concentration in DMSs should not exceed 2×10^{18} cm⁻³. Our description of BMP hopping accounts for the thermodynamic fluctuations and clearly ignores the quantum fluctuations of the magnetizations. The latter will be shown not to be important for the materials in question

down to temperatures as low as 0.1 K. We will address this issue in the end of Sec. IV where BMP hopping conductivity is discussed.

In performing the functional integration in Eqs. (10) and (13), it is convenient to replace it with an ordinary integration over $\vec{\Delta}$ and $\vec{\Delta}'$ by means of the following obvious representation of the integrands in Eqs. (10) and (13):

$$\Phi(\vec{\Delta}_1, \vec{\Delta}_2) = \int \int \Phi(\vec{\Delta}, \vec{\Delta}') \delta(\vec{\Delta} - \vec{\Delta}_1 \{ \vec{M}_1(\vec{r}) \}) \times \delta(\vec{\Delta}' - \vec{\Delta}_2 \{ \vec{M}_2(\vec{r}) \}) d\vec{\Delta} d\vec{\Delta}'. \quad (14)$$

It finally yields

$$w_{12} = \frac{2\pi}{\hbar Z_i'} \sum_{\sigma_1, \sigma_2} \int \int |\bar{t}_{\sigma_1 \sigma_2}|^2 \times \exp\left(\frac{\sigma_1 \Delta/2 - \epsilon_1}{T}\right) P_1(\vec{\Delta}) P_2(\vec{\Delta}') \times f\left(\epsilon_{12} - \frac{\sigma_1 \Delta - \sigma_2 \Delta'}{2}\right) d\vec{\Delta} d\vec{\Delta}', \quad (15)$$

where $\epsilon_{12} = \epsilon_1 - \epsilon_2$,

$$Z_i' = 2 \exp\left(-\frac{\epsilon_1}{T}\right) \int P_1(\vec{\Delta}) \cosh(\Delta/2T) d\vec{\Delta} \int P_2(\vec{\Delta}') d\vec{\Delta}' \quad (16)$$

is the normalization factor, and

$$P_l(\vec{\Delta}) = \int \mathcal{D}\vec{M}_l \delta(\vec{\Delta} - \vec{\Delta}_l \{ \vec{M}_l(\vec{r}) \}) \times \exp\left(-\frac{1}{2\chi T} \int \delta\vec{M}_l^2(\vec{r}) d\vec{r}\right) \quad (17)$$

is a distribution function of the spin-splitting vectors in the absence of a localized electron. The functional integral (17) is of the Gaussian type. It was calculated by Dietl and Spáček (DS):¹⁰

$$P_l(\vec{\Delta}) \propto \exp\left[-\frac{(\vec{\Delta} - \vec{\Delta}_0)^2}{16W_{p,l}T}\right], \quad (18)$$

where

$$\vec{\Delta}_0 = \frac{\Gamma_{ex}}{g\mu_B} \vec{M}_0 + g^* \mu_B \vec{B} \quad (19)$$

is the equilibrium value of the Zeeman splitting vector in absence of a localized electron. In Eq. (18), the polaron shift $W_{p,l}$ was introduced:

$$W_{p,l} = \left(\frac{\Gamma_{ex}}{2g\mu_B}\right)^2 \frac{\chi(B, T)}{2} \int |\Psi_l(\vec{r})|^4 d\vec{r} \equiv \left(\frac{\Gamma_{ex}}{2g\mu_B}\right)^2 \frac{\chi(B, T)}{2\Omega_l}, \quad (20)$$

which is half the electronic part of the polaron shift $\epsilon_p = 2W_p$ considered by DS.¹⁰ In Eq. (20), we defined an effective volume Ω_l of a BMP as

$$\Omega_i^{-1} \equiv \int |\Psi_i(\vec{r})|^4 d\vec{r}. \quad (21)$$

In calculating the hopping conductivity in Sec. IV we will need the rate of BMP hopping between two almost identical sites that belong to a percolation cluster. That is why in all the further considerations we will assume that $\Omega_1 \approx \Omega_2 \approx \Omega$ and $W_{p,1} \approx W_{p,2} \approx W_p$.

It is important to mention that our major result (15) is more general than it appears at first sight. If the distribution function (17) is defined as a quantum-statistical average over the discrete atomic spins rather than a functional integral over the classical magnetization field (see Appendix A for details), then formula (15) is still valid and goes beyond the Gaussian approximation. In particular, as demonstrated in Appendix A, in the limit of zero magnetic field this formula reproduces the results of the Nagaev-Podel'schikov¹⁴ (NP) model.

The Gaussian form of the distribution function (18), leads

to Gaussian-type integrals in Eq. (15). In this case the BMP hopping rate (15) can be calculated analytically, yielding

$$w_{12} = \frac{\sqrt{\pi}|t|^2}{2\hbar T} (p_{12}^{(0)} + p_{12}^{(ph,+)} + p_{12}^{(ph,-)}), \quad (22)$$

where

$$p_{12}^{(0)} = F(\mu, \nu; \eta_0) \exp\left[-\frac{(2W_p - \epsilon_{12})^2}{8W_p T}\right] \quad (23)$$

and

$$p_{12}^{(ph,\pm)} = \sum_q |\Lambda_q|^2 \left(N_q + \frac{1}{2} \mp \frac{1}{2}\right) F(\mu, \nu; \eta_{\pm}) \times \exp\left[-\frac{(2W_p - \epsilon_{12} \mp \hbar\omega_q)^2}{8W_p T}\right], \quad (24)$$

where

$$F(\mu, \nu; \eta) = (\mu\sqrt{\nu})^{-1} \left[\frac{(\mu^2 - \eta^2 + 2) \cosh \mu + 2(\eta \sinh \eta - \cosh \eta) \exp(-\nu)}{2(\mu \sinh \mu + \nu \cosh \mu)} + 2\nu - 1 \right] \quad (25)$$

and the following dimensionless parameters were introduced: $\mu = \Delta_0/2T$, $\nu = \Delta_0^2/8W_p T$, $\eta_0 = \Delta_0 \epsilon_{12}/4W_p T$, and $\eta_{\pm} = \Delta_0(\epsilon_{12} \pm \hbar\omega_q)/4W_p T$. Here Δ_0 is given by Eq. (19).

The expression (25) corresponds to the hopping integral given by Eq. (9) which, in turn, is derived assuming that there are no spin-flip processes. If, however, the latter assumption is relaxed (e.g., the probabilities of spin-flip and non-spin-flip processes are equal), then the hopping integral $\bar{t}_{\sigma,\sigma'}$ does not depend on the angles. In this case, the prefactor F in Eq. (23) should be replaced by

$$\begin{aligned} \bar{F}(\mu, \nu; 0) &= (\mu\sqrt{\nu})^{-1} \\ &\times \left[\frac{(\mu^2 + 2\nu)[\cosh \mu - \exp(-\nu)]}{2(\mu \sinh \mu + \nu \cosh \mu)} + 2\nu \right]. \end{aligned} \quad (26)$$

In the general expression (22), the first term (23) represents the resonant transitions. In the case of sufficiently large magnetic fields ($B \rightarrow \infty$) the angular fluctuations of the magnetizations are effectively suppressed. That implies that $W_p \rightarrow 0$ ($\chi \rightarrow 0$ as $B \rightarrow \infty$) while Δ_0 approaches its saturation value $\Delta_s \gg |\epsilon_{12}|$. Then $F(B \rightarrow \infty) = (2T/W_p)^{1/2}$ and therefore the resonant part of the BMP hopping rate

$$\begin{aligned} w_{12}^{(0)}(B \rightarrow \infty) &= \frac{\sqrt{\pi}|t|^2}{2\hbar T} p_{12}^{(0)}(B \rightarrow \infty) \\ &= \frac{|t|^2}{\hbar} \left(\frac{\pi}{2W_p T}\right)^{1/2} \exp\left[-\frac{(2W_p - \epsilon_{12})^2}{8W_p T}\right], \end{aligned} \quad (27)$$

which coincides with the basic result of the conventional theory of small lattice polarons.¹⁵

The last two terms in Eq. (22) describe the transitions with the absorption and emission of acoustical phonons, respectively. They are analyzed in Appendix B where it is shown that if the polaron shift W_p is much greater than the scatter in the ‘‘bare’’ energies ϵ_{12} , the resonant tunneling prevails over the phonon-assisted one. Otherwise, the standard Miller-Abrahams^{19,21} expression (B7) for the hopping rate can be obtained from Eq. (22).

IV. BMP HOPPING CONDUCTIVITY

Using the standard technique of the percolation theory^{19,21} and expression (22) for the hopping probability one can calculate the effective electrical hopping resistance between sites i and j :

$$R_{ij} = \frac{T}{e^2 w_{ij} f_i (1 - f_j)}, \quad (28)$$

where $f_i = \{1 + \exp[(\epsilon_i - E_F)/T]\}^{-1}$ is Fermi's distribution function of the localized electrons with the Fermi level E_F . Therefore,

$$R_{ij} \propto F^{-1}(\mu, \nu; 0) \exp\left(\frac{2r_{ij}}{a} + \frac{\tilde{\epsilon}_{ij}}{T}\right), \quad (29)$$

where r_{ij} is the distance between the sites in question and

$$\begin{aligned} \tilde{\epsilon}_{ij} &= \frac{1}{2} (|\epsilon_i - E_F| + |\epsilon_j - E_F|) \\ &+ \begin{cases} W_p/2 + (\epsilon_i - \epsilon_j)^2/(8W_p), & |\epsilon_i - \epsilon_j| \leq 2W_p, \\ |\epsilon_i - \epsilon_j|/2, & |\epsilon_i - \epsilon_j| > 2W_p. \end{cases} \end{aligned} \quad (30)$$

With the exception of a very important magnetic-field-dependent factor F^{-1} , expression (29) coincides with that of Ref. 13. This factor, which is specific for BMP hopping, takes into account the vector nature of the magnetic order parameter. We will show that it is responsible for the *positive* magnetoresistance observed at small and intermediate magnetic fields in different magnetic semiconductors and nanostructures.^{6,18} The interpolation formula (29) takes into account two limiting cases of (i) large polaron shifts $2W_p > \langle |\epsilon_{ij}| \rangle$, which is appropriate for the BMP with an appreciable polaron shift when the magnetic field is not strong, and (ii) small polaron shifts $2W_p < \langle |\epsilon_{ij}| \rangle$ when it is strong (see Appendix B for details). Here $\langle |\epsilon_{ij}| \rangle = \langle |\epsilon_i - \epsilon_j| \rangle$ is an average scatter of the ‘‘bare’’ electron energies.

While evaluating the hopping resistivity ρ we will consider the case of ϵ_3 conductivity²¹ when the typical dispersion of the activation energies $\tilde{\epsilon}_{ij}$ is small compared to that of the intersite distances r_{ij} , namely, $\langle \tilde{\epsilon}_{ij} \rangle / T \ll 2 \langle r_{ij} \rangle / a$. In this case the connectivity criterion can be written as

$$\frac{2r_{ij}}{a} + \frac{\tilde{\epsilon}_{ij}}{T} \leq \xi_c = \frac{2r_c}{a} + \frac{\langle \tilde{\epsilon}_{ij} \rangle}{T}, \quad (31)$$

where r_c is a percolation threshold for the random-site r -percolation problem.²¹ (Usually r_c is of the order of the average distance between sites.) It yields the following expression for the resistivity:

$$\rho(B) \propto F^{-1}(\mu, \nu; 0) \exp\left(\frac{2r_c}{a} + \frac{\epsilon_3}{T}\right), \quad (32)$$

where

$$\epsilon_3 = \epsilon_3^{MA} + \frac{W_p}{2} f(\alpha). \quad (33)$$

Here ϵ_3^{MA} is the activation energy for the Miller-Abrahams hopping conductivity in the absence of the BMP effect, $\alpha = 2W_p / \delta$ where δ is a typical scatter of electron energies, and $f(\alpha)$ is a dimensionless function such that $f(\alpha) \rightarrow 0$ when $\alpha \ll 1$ and $f(\alpha) \rightarrow 1$ when $\alpha \gg 1$. Both ϵ_3^{MA} and $f(\alpha)$ are evaluated in Appendix C for a simple rectangular distribution function of electron energies ϵ . It should be noted that the activation energy for the magnetoresistance, Eq. (32), driven by the fluctuations of local magnetization, is one-fourth the value obtained for the static BMP states.^{6,12} Therefore, the fluctuation-driven mechanism of hopping will always dominate over the static one.¹³

Thus, we have established that the fluctuation-driven scenario of BMP hopping leads to the exponential dependence (32) of the magnetoresistance with an activation energy (33) that strongly depends on the magnetic field through the polaron shift W_p . Comparison with the experimental data for DMS's and Er-based nanostructures supports this conclusion (see Sec. VI for details). Contrary to this statement, quantum fluctuations of magnetizations would manifest themselves in the field-independent activation energy of the magnetoresistance, which obviously contradicts the experimental data in question. This fact was explained by Iosevich¹³ who mentioned that disordered magnets are characterized by extremely slow relaxation of the magnetization.²² Direct

measurements^{23,24} show that, for instance, in $\text{Cd}_{1-x}\text{Mn}_x\text{Te}$ the BMP formation rate at $T = 1-2$ K is $\tau_R^{-1} \approx 0.1$ K, i.e., $\tau_R \approx 400$ ps. This means that the characteristic pseudomagnon frequencies are of the order of 0.1 K, and therefore, the contribution from quantum fluctuations to the BMP hopping rate is negligibly small if $T > \tau_R^{-1}$.¹³

V. MAGNETORESISTANCE

To analyze the field dependence of the magnetoresistance (32), one should specify the magnetic susceptibility $\chi(B, T)$. Usually, for dilute magnetic semiconductors in the paramagnetic phase,^{6,10,11} it can be expressed in terms of a modified Brillouin function $B_J(z)$:⁶

$$B_J(z) = \frac{1}{2J} \left[(2J+1) \coth\left(\frac{(2J+1)z}{2}\right) - \coth\left(\frac{z}{2}\right) \right]. \quad (34)$$

The magnetic susceptibility can then be written as

$$\chi(B, T) = \frac{\partial M_0}{\partial B} = \frac{3}{J+1} B'_J(z) \chi(0, T), \quad (35)$$

where

$$\chi(0, T) = \frac{(g\mu_B)^2 n_0 J(J+1)}{3(T+T_0)} \quad (36)$$

is a zero-field susceptibility that obeys a modified Curie's law and n_0 is the concentration of magnetic atoms. Here $z = g\mu_B B / (T+T_0)$ and the parameter $T_0 > 0$ is associated with the possible antiferromagnetic interaction of magnetic atoms with the total angular momentum J and Lande factor g . Then the average Zeeman splitting (19) in the absence of a localized electron is

$$\Delta_0(B) = n_0 \Gamma_{ex} J B_J(z) = \Delta_s B_J(z), \quad (37)$$

where

$$\Delta_s = \Delta(B \rightarrow \infty) = n_0 \Gamma_{ex} J \quad (38)$$

is the splitting at saturation fields. In deriving Eqs. (37) and (38) we have ignored the direct input from the external magnetic field because it is usually several orders of magnitude smaller than that of the exchange field. Now the polaron shift can be rewritten as

$$W_p(B) = \frac{\chi(B)}{\chi(0)} W_p(0) = \frac{3}{J+1} B'_J(z) W_p(0). \quad (39)$$

It clearly tends to zero as the magnetic field approaches its saturation value, and

$$W_p(0) = \left(\frac{\Gamma_{ex}}{2g\mu_B} \right)^2 \frac{\chi(0, T)}{2\Omega} = \frac{\Gamma_{ex}^2 n_0 J(J+1)}{24(T+T_0)\Omega} \quad (40)$$

is the polaron shift at zero magnetic field. From here it follows [see Eq. (33)] that when the typical scatter of electron energies $\delta \ll W_p(0)$ the magnetic part of the activation energy of hopping resistivity is close to $W_p(0)/2$. If the antiferromagnetic interaction is negligibly small ($T_0 = 0$), this result also can be obtained from the formula derived by NP (Ref. 14) (see Appendix A).

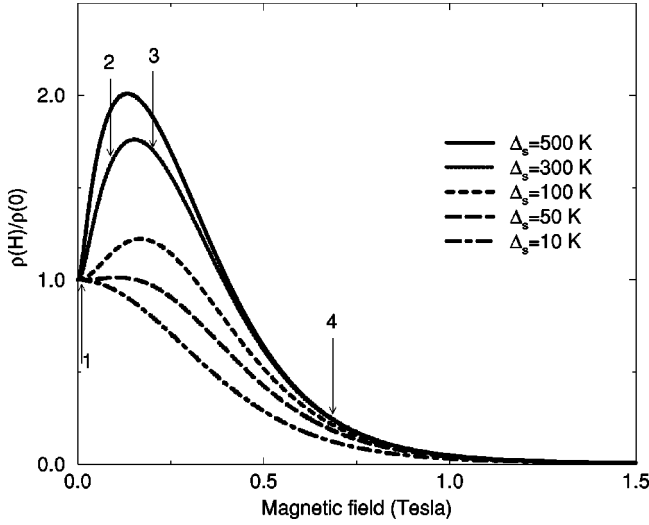


FIG. 1. Field dependence of the BMP hopping magnetoresistance, Eq. (32), for the following set of parameters: $W_p(0) = 24.2$ K, $J = 3/2$, $g = 2$, $T_0 = 4$ K, $T = 1.5$ K, $\delta = 0$, and different values of the saturation splittings Δ_s [Eq. (38)].

Figure 1 shows the magnetic-field dependence of the BMP hopping resistivity calculated by means of Eq. (32) for different values of saturation splitting Δ_s . It displays the overall drop in the resistivity with the magnetic field that clearly reflects the decrease in the polaron shift and in the typical hopping barrier $W_p(B, T)/2\alpha\chi(B, T)$. The scale of this effect exponentially depends [see Eq. (32)] on the ratio of $W_p(0)/T$ and can easily reach several orders of magnitude at low temperatures in materials with appreciable polaron shifts.^{8,10,18}

However, at relatively small fields the resistivity can significantly increase (up to several times) with the field. Our calculations (Fig. 1) show that this giant positive magnetoresistance can be observed when $\Delta_s^2/W_p(0)T \geq 1$. It is governed by a sharp decrease in the field dependence of factor F , Eq. (25), that controls the number of states available for resonant tunneling. In other words, the effect in question is connected with a field-induced suppression of the fluctuations of the angles between the local magnetization, mainly on the occupied site, and the applied magnetic field.

In order to demonstrate this, we have evaluated the distributions $g_1 = a_1 P(\vec{\Delta}) \cosh(\Delta/2T)$ and $g_0 = a_0 P(\vec{\Delta})$ of the Zeeman splitting vectors $\vec{\Delta}$, respectively, at sites with and without BMP and displayed them in Fig. 2. Here $P(\vec{\Delta})$ is given by Eq. (18), and a_1 and a_0 are normalization factors. For the sake of simplicity, let us ignore the angular dependence of the transfer integral (9) as it is not essential here. We also suppose that $\epsilon_{12} = 0$. Then the resonant BMP hopping rate between the occupied and empty sites in question is obviously proportional to an overlap integral of the above-mentioned distributions:

$$w_{12}^{(0)} \propto \int d\vec{\Delta} g_1(\vec{\Delta}) g_0(\vec{\Delta}), \quad (41)$$

represented by the shaded areas in Fig. 2. It can be seen that initially, at zero field, the fluctuations at both sites with all possible directions of local magnetizations (vectors $\vec{\Delta}$) are

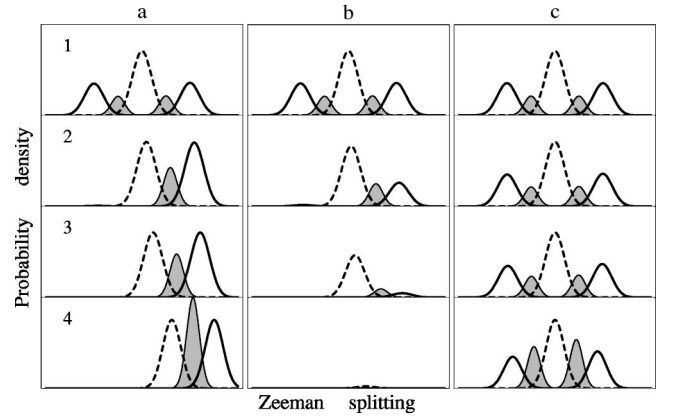


FIG. 2. Distributions of Zeeman splitting vectors $\vec{\Delta}$ at a site occupied by a BMP (solid lines) and an “empty” site (dashed lines) for the four magnetic fields, directed to the right, indicated by arrows in Fig. 1. For (a) and (b) $\Delta_s = 300$ K; for (c) $\Delta_s = 10$ K where Δ_s is the saturated splitting. The distributions are given along the lines crossing the origin in the direction of the magnetic field [(a) and (c)] and at 45° with respect to the magnetic field (b). The shaded areas represent the overlap of the distributions greatly increased in magnitude to make it visible.

equally available for hopping. Then, after a magnetic field is applied, in the case when $\Delta_s^2/W_p(0)T \geq 1$, the fluctuations of the magnetization at the occupied sites, which are directed mainly against the field, cease to contribute to the conductivity. [The left-hand maxima of the corresponding distributions shown in sets (a) and (b) tend to collapse with increasing field.] Meanwhile, the fluctuations with the magnetizations directed along the field play an increasingly greater role. If the field is small enough ($B \leq 0.15$ T) and $\Delta_s^2/W_p(0)T \geq 1$, the first process prevails over the second one, thus *decreasing* the hopping probability (41) and, therefore, increasing the resistivity. In other words, if the BMPs have sizable self-induced magnetic moments that are randomly oriented at zero magnetic field, a relatively small external magnetic field will almost immediately align them mainly along its direction provided that $\Delta_s^2/W_p(0)T \geq 1$. Later on, at higher fields, the hopping probability begins to rise with the field due to lowering of the polaron hopping barrier.

So the appearance of the maximum in the field dependence of resistivity can be seen as a signature of the fluctuation-driven BMP hopping connected with the vector nature of the fluctuating order parameter. The application of a relatively small magnetic field suppresses the fluctuations of the local magnetizations both in magnitude and direction. The maximum results from the interplay of these two factors. The first factor always leads to the giant negative magnetoresistance that occurs when large fields are applied, while the second one, under certain conditions, may be responsible for a quite sizable positive magnetoresistance. In the following section, we will show that these effects are indeed seen in some dilute magnetic semiconductors and magnetic nanostructures.

VI. COMPARISON WITH EXPERIMENT

A. Dilute magnetic semiconductors

Both positive and negative magnetoresistance have been experimentally observed in the insulating region in several

II-VI semiconductors, such as CdSe, HgTe, CdHgTe, and ZnSe, doped to high (up to several atomic percent) concentrations with transition metals, mainly, with Mn. For p -type materials, several, sometimes controversial, explanations of these phenomena were put forward (see Ref. 6 and references therein) that are based on the complex nature of localized acceptor states involved.⁶ To avoid unnecessary complications, we will restrict ourselves to a case of n -doped $\text{Cd}_{0.95}\text{Mn}_{0.05}\text{Se}$, where donors, on which the magnetic polarons reside, can be described by means of a simple hydrogenlike model. [A detailed and consistent theory of the BMPs in this material was developed by Dietl and Spáček¹⁰ who successfully applied it to a description of the experiments on spin-flip Raman scattering (see also Ref. 11).] Later on, the BMP hopping conduction was studied experimentally in these materials.¹² However, the theoretical interpretation of these experiments given in Ref. 12 was based on a static model that grossly overestimates the magnetoresistance. We will analyze these experiments in terms of the above-developed fluctuation-driven hopping model.

We start our analysis from the experimental data (Fig. 1 from Ref. 12) on the temperature dependence of the resistivity (measured at zero magnetic field and at the magnetic field $B=6$ T that is close to saturation) of two $\text{Cd}_{0.95}\text{Mn}_{0.05}\text{Se}$ samples (a) and (b) with different donor concentrations equal to $6 \times 10^{16} \text{ cm}^{-3}$ and $1.2 \times 10^{17} \text{ cm}^{-3}$, respectively. It should be noted that these dependences are of the activation type with the activation energy decreasing with magnetic field. This fact clearly indicates that BMP hopping is driven by the thermodynamic rather than quantum fluctuations of magnetization. Then, by means of our basic formula (32), taken at $B=0$ and $B \rightarrow \infty$ [when the polaron shift $W_p(B) \rightarrow 0$], we extracted the values of the zero-field polaron shift $W_p(0)$ from these data to be close to 16.4 and 9.0 K for samples (a) and (b), respectively. These shifts together with $\Delta_s=180$ and the parameters $T_0=1.2$ K, $g=2$, and $J=5/2$ (Ref. 10) for the modified Brillouin function (34) were used to plot the calculated magnetoresistance (32) of DMSs (Fig. 3) for $T=1.7$ and 4.2 K where it is compared with the experimental data from Ref. 12. In calculating the magnetoresistance (32) we used the expressions (25) (spin flips are forbidden) and (26) (spin-flip processes are allowed). It can be seen that the latter one leads to a better agreement with the experiment.

A few comments should be made as to possible sources of discrepancies between the theory and experiment as well as between the optical¹⁰ and electrical¹² data. The samples under consideration are close to the metal-insulator transition (MIT) point¹² where the spatial fluctuations of the donor concentration are large enough. First of all, it explains why the above-obtained zero-field polaron shifts (≈ 16 and 9 K), which for a simple hydrogenlike model [see Ref. 10 and Eq. (20)], where $\Omega \approx 16\pi a^3$ with a being the localization radius of the BMP), are equal to

$$W_p(0) = \left(\frac{\Gamma_{ex}}{2g\mu_B} \right)^2 \frac{\chi(0)}{32\pi a^3}, \quad (42)$$

are several times greater than that (≈ 2 K) extracted from the optical experiments.¹⁰ Indeed, for the ϵ_3 -percolation model,²¹ which seems to work here, the states effectively

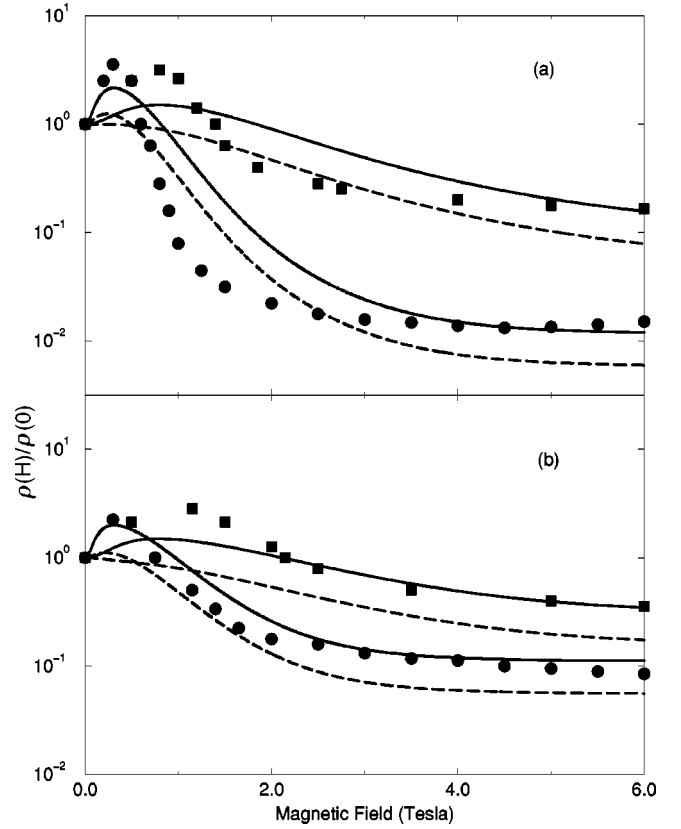


FIG. 3. Magnetoresistance of $\text{Cd}_{0.95}\text{Mn}_{0.05}\text{Se}$ for various donor concentrations n : (a) $6 \times 10^{16} \text{ cm}^{-3}$, (b) $1.2 \times 10^{17} \text{ cm}^{-3}$. The circles and squares represent the experimental data (Ref. 12) taken at $T=1.7$ and 4.2 K, respectively. The solid and dashed lines represent the theoretical results obtained with and without spin-flip processes taken into account, respectively, with the following set of parameters: (a) $W_p(0)=16.4$ K, $\delta=3.6$ K, $E_F=3.4$ K; (b) $W_p(0)=9.0$ K, $\delta=4.2$ K, $E_F=0.9$ K.

involved in the hopping conduction belong to the peak in the energy distribution $n(\epsilon)$ that describes the impurity band. These states originate from the donors that are quite well separated from each other with comparatively small localization radii and, therefore, with rather large polaron shifts (42). On the other hand, the states involved in optical absorption are close to the Fermi level, which lies in the band tail of the impurity band. These states originate from large-scale fluctuation of the impurity potential; i.e., they are associated with aggregations of several donors.²¹ Therefore, the localized electron function is spread over somewhat (4–7 times) greater volume than that of the isolated donors; i.e., its effective localization radius is from 1.5 to 2 times greater. As a result, the polaron shift is correspondingly lower than that typical for the resistivity measurements.

Moreover, with its higher donor concentration, sample (b) is closer to the MIT point where the spatial fluctuations of the impurity potential are large. Here, in accordance with the percolation theory,²¹ even the states that are in the vicinity of the energy-distribution peak reveal the tendency to coalesce. The donors will often form di- or tri-atomic ‘‘molecules,’’ thus increasing the effective localization radius. This explains (i) why the polaron shift of sample (b) is smaller than that of sample (a) (see Fig. 3) and (ii) why our simple iso-

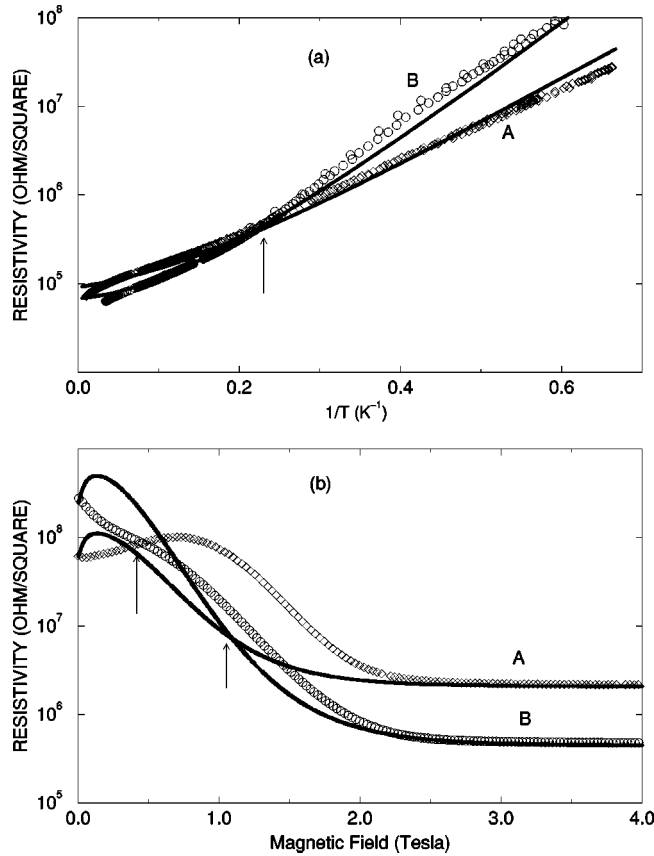


FIG. 4. Resistivity of the ErAs/GaAs nanostructures as a function of (a) temperature and (b) magnetic field perpendicular to the direction of growth at $T=1.7$ K (Ref. 18). Diamonds represent sample A; circles represent sample B. Solid lines are theoretical results.

tropic model fails to describe all the details in the field dependence of the BMP hopping resistivity in $Cd_{0.95}Mn_{0.05}Se$.

B. ErAs/GaAs magnetic nanostructures

Recently, the molecular beam epitaxy (MBE) technique has been used to grow self-assembled nanometer-sized ErAs magnetic islands (quantum dots) embedded in a semi-insulating GaAs matrix when the amount of material deposited in the ErAs layers ranged from 0.5 to 2.5 molecular layers (ML).¹⁸ Precise control of the deposition conditions made it possible to control not only the concentration of these islands and interisland distance but their size, which ranged from 4 to 80 nm. Analysis of the temperature dependence of the zero-field resistivity together with the data on the magnetoresistance for different samples clearly shows that the low-temperature conductivity in these materials can be explained in the framework of fluctuation-driven BMP hopping.^{7,18}

In the analysis of the data on magnetoresistance¹⁸ we used the modified Brillouin function (34) to fit the experimental data on magnetization and susceptibility (35) with the spin and g factor of the Er ions $J=3/2$ (Ref. 25) and $g=7.4$, and with the effective temperature describing antiferromagnetic interaction, $T_0=4$ K. One can see that formula (32) describes the temperature dependence of the zero-field resistivity [Fig. 4(a)] well in the temperature range relevant to the

experimental data. Here, like that of DMSs, the activation energy of the magnetoresistance is a decreasing function of magnetic field.⁷ This again is a direct signature of BMP hopping driven by thermodynamic fluctuations of magnetization. We used the following values of the zero-field polaron shifts, $W_p(0)=24.2$ K and 17.4 K, and of the scatters of the electron energies, $\delta=15.0$ K and 22.2 K, respectively, for samples B and A to fit the theoretical temperature dependences of the zero-field resistivity to the experimental ones.¹⁸ The data shown in this figure correspond to samples A and B grown at the same 2-ML ErAs depositions and at different temperatures. Sample B (see Fig. 4) with islands of smaller lateral size d than that of sample A has a smaller average distance \bar{r} between them. The observed crossover results from competition between the activation energy term (which increases as the islands' size decreases) and the hopping integral term (which decreases as the separation between the islands decreases) in expression (32). At low temperatures the activation term prevails, while at high temperatures the conductivity is governed by activationless r hopping. (This crossover can be reversed at low temperatures by applying magnetic field that quenches the activation energy [see Fig. 4(b)]. The theoretical curves in Fig. 4 were calculated for a typical lateral size of the islands, $d\approx 50$ Å ($W_p=17.4$ K) and 40 Å ($W_p=24.2$ K), for samples A and B, respectively, which is consistent with transmission electron microscope (TEM) observations.¹⁸ We used the Zeeman splitting at saturation, $\Delta_s=50$ meV. Relatively small ($<20\%$) changes in d have a dramatic effect not only on the zero-field resistivity but also on the scale of the negative magnetoresistance. In accordance with our model, the latter definitely correlates with the islands' size d and volume $V\approx\Omega_0$ and, therefore, with the magnitude of the zero-field polaron shift (40), $W_p(0)\sim 1/V$ [see Fig. 4(b)]. At intermediate fields, the resistivity as a function of magnetic field B may reveal a maximum the origin of which has been explained in Sec. V.

The experimental curves^{7,18} clearly display a dependence of the magnetoresistance on the orientation of magnetic field that cannot be explained in the framework of our simple isotropic model. A few factors may contribute to this effect, such as the anisotropy of the magnetization and the anisotropy in the shape and size of the islands that can interplay with the complex nature of the confined electronic states to cause an anisotropy of the exchange coupling (as was observed for the hole states in ErAs quantum wells^{26,27}).

A comment is in order as to a possible role of the charging energy in the description of the hopping conductivity in ErAs/GaAs nanocomposites. For islands with dimensions of 40–50 Å, this energy is of the order of 200 K. That is much larger than all the characteristic energies involved including a residual high-magnetic-field activation energy which is of the order of $|E_F|+\delta/6\approx 2-3$ K. A possible explanation for this is that the conductivity is due to the carriers moving in an almost unoccupied upper (for electrons) or lower (for holes) Hubbard band. These carriers might be supplied by a small uncontrolled concentration of dopants in the GaAs matrix. However, it is more likely that the Fermi level E_F is pinned by overlapping density of states (DOS) of the band tails that originate from the electron and holelike localized states of the semimetallic ErAs islands. If it is true, then it can be shown that, due to a significant difference in the ef-

fective masses of electrons and holes, the Fermi level can be shifted from the center of a charging-energy gap towards a subband with larger DOS, thus leading to a residual activation energy that is much smaller than the charging energy and that does not depend on the concentration of the uncontrolled dopants.

VII. CONCLUSIONS

A simple theory of the bound magnetic polaron hopping driven by the fluctuations of local magnetizations gives a reasonably good explanation, both qualitative and quantitative, of the experimental data on giant negative and positive magnetoresistance in dilute magnetic semiconductors and nanostructures. Future refinements of the theory of the BMP hopping presented in this paper should incorporate magnetic-field orientation effects that are believed to be connected with the shape anisotropy of magnetic nanostructures.

ACKNOWLEDGMENTS

This work was supported by AFOSR Grant No. F49620-96-1-0383. The authors are grateful to S. J. Allen, D. Schmidt, B. Segall, and R. L. Corey for numerous fruitful discussions.

APPENDIX A: COMPARISON WITH THE s - d MODEL

Let us start from the standard s - d spin Hamiltonian^{11,14}

$$H_k^{(s-d)} = \epsilon_k n_k + H_k(\{\vec{J}_k\}) - \vec{s}_k \left(\Gamma_{ex} \sum_l |\Psi(\vec{R}_l)|^2 \vec{J}_{k,l} + g \mu_B \vec{B} \right) \equiv \epsilon_k n_k + H_k - \vec{s}_k \vec{\Gamma}_k, \quad (\text{A1})$$

where Γ_{ex} is the exchange coupling constant and $\Psi(\vec{R}_l)$ is the electron wave function at the atomic site l . Equation (A1) describes the exchange interaction of an electron, localized at the BMP site k ($k=1,2$), with atomic spins $\vec{J}_{k,l}$ in the vicinity of this electron; i.e., \vec{s}_k and $\vec{\Gamma}_k$ are operators of the electron spin and atomic exchange field, respectively. The Hamiltonians H_k describe interactions of the atomic spins with each other and with the external magnetic field \vec{B} . The explicit form of H_k is not important for further derivation. In order to calculate the hopping probability by means of Fermi's golden rule, we assume that in the initial ($|i\rangle$) and final ($|f\rangle$) states of the system the electron is fully spin polarized and forms BMPs on sites 1 and 2, respectively. Introducing initial ($\vec{\nu}_1$) and final ($\vec{\nu}_2$) spin-quantization axes we can represent $|i\rangle$ and $|f\rangle$ as

$$|i\rangle = |\vec{\nu}_1 \sigma_1\rangle |2\rangle b_{1\sigma_1}^\dagger |0\rangle, \quad (\text{A2a})$$

$$|f\rangle = |\vec{\nu}_2 \sigma_2\rangle |1\rangle b_{2\sigma_2}^\dagger |0\rangle. \quad (\text{A2b})$$

Here $\sigma_k = \pm 1$, $|\vec{\nu}_k \sigma_k\rangle$ and $|k\rangle$ are the eigenvectors of the operators $H_k - \sigma_k \vec{\nu}_k \vec{\Gamma}_k / 2$ and H_k , respectively, $|0\rangle$ is the vacuum state, and operators $b_{k\sigma_k}^\dagger$ are given by Eq. (7) with the angles pertaining to the unit vectors $\vec{\nu}_k$.

The assumption (A2) allows us to calculate the matrix elements of the operator H_{12} [Eq. (5)] between the initial and final states. As a result, Fermi's golden rule can be presented in the following form:

$$w_{12} = \frac{2\pi}{\hbar Z} \sum_{i,f} |\langle i | H_{12} | f \rangle|^2 \exp(-\beta E_i) \delta(E_f - E_i) = \frac{2\pi}{\hbar Z} \sum_{\sigma_1 \sigma_2} \sum_{\nu_1 \nu_2} \sum_{pqrs} |\bar{t}_{\sigma_1 \sigma_2}|^2 \exp[-\beta(\epsilon_1 + E_{\nu_1 \sigma_1}^{(p)} + E_2^{(q)})] |\langle \vec{\nu}_1 \sigma_1^{(p)} | 1^{(s)} \rangle \langle 2^{(q)} | \vec{\nu}_2 \sigma_2^{(r)} \rangle|^2 \delta(\epsilon_{12} + E_{\nu_1 \sigma_1}^{(p)} + E_2^{(q)} - E_{\nu_2 \sigma_2}^{(r)} - E_1^{(s)}), \quad (\text{A3})$$

where $\beta = 1/T$, indices p, q, r, s enumerate corresponding eigenstates, and $|\bar{t}_{\sigma_1 \sigma_2}|^2$ is given by Eq. (9) with θ_{12} being the angle between $\vec{\nu}_1$ and $\vec{\nu}_2$; $E_{\nu_k \sigma_k}$ and E_k are eigenvalues of the operators $H_k - \sigma_k \vec{\nu}_k \vec{\Gamma}_k / 2$ and H_k , respectively; $\epsilon_{12} = \epsilon_1 - \epsilon_2$. Here, for the sake of simplicity we neglected direct contributions from single-phonon processes. Using completeness of the states $|\vec{\nu}_2 \sigma_2\rangle |1\rangle$ and the Fourier representation of the δ function in Eq. (A3), we obtain

$$w_{12} = \frac{2\pi}{\hbar Z} \sum_{\sigma_1 \sigma_2} \sum_{\nu_1 \nu_2} |\bar{t}_{\sigma_1 \sigma_2}|^2 \int_{-\infty}^{\infty} \frac{d\lambda}{2\pi} \text{Tr} \exp[-\beta H_1 - (\beta - i\lambda) \times (\epsilon_1 - \sigma_1 \vec{\nu}_1 \vec{\Gamma}_1 / 2)] \times \text{Tr} \exp[-\beta H_2 - i\lambda (\epsilon_2 - \sigma_2 \vec{\nu}_2 \vec{\Gamma}_2 / 2)]. \quad (\text{A4})$$

As a next step we define two Zeeman splitting vectors $\vec{\Delta} = \Delta \cdot \vec{\nu}_1$ and $\vec{\Delta}' = \Delta' \cdot \vec{\nu}_2$ and use the approximation, first introduced in Ref. 11,

$$g(\vec{\Gamma}) = \int \delta(\vec{\Delta} - \vec{\Gamma}) g(\vec{\Delta}) d\vec{\Delta}, \quad (\text{A5})$$

where $g(\vec{\Gamma})$ is an arbitrary function of the operator $\vec{\Gamma}$. It finally yields

$$w_{12} = \frac{2\pi}{\hbar Z_i} \sum_{\sigma_1, \sigma_2} \int \int |\bar{t}_{\sigma_1 \sigma_2}|^2 \times \exp\left(\frac{\sigma_1 \Delta / 2 - \epsilon_1}{T}\right) \tilde{P}_1(\vec{\Delta}) \tilde{P}_2(\vec{\Delta}') \times \delta\left(\epsilon_{12} - \frac{\sigma_1 \Delta - \sigma_2 \Delta'}{2}\right) d\vec{\Delta} d\vec{\Delta}'. \quad (\text{A6})$$

Equation (A6) coincides with formula (15) except that here we omitted the acoustic phonon contribution. Also we replaced $P_k(\vec{\Delta})$, Eq. (17), with

$$\tilde{P}_k(\vec{\Delta}) = \text{Tr}[\exp(-\beta H_k) \delta(\vec{\Delta} - \vec{\Gamma}_k)]_{\{\vec{j}_k\}}, \quad (\text{A7})$$

which are defined as quantum-mechanical expectation values, rather than the functional integrals over the classical magnetization fields.

The approximation (A5) is valid if the number of atomic spins, N , within the localization volume Ω of the BMP is large enough ($N^{1/2} \gg 1$).¹¹ Under the same circumstances and when the magnetization is far from saturation, the distribution functions $\tilde{P}_k(\vec{\Delta})$ are Gaussian and are given by Eq. (18).¹¹ They remain Gaussian (but temperature independent) even if $H_k=0$, i.e., when Eq. (18) is evaluated with the Curie-Weiss magnetic susceptibility.

In order to match our results with those of NP,¹⁴ we set $\bar{t}_{\sigma_1\sigma_2}=t_0$, $\epsilon_{12}=0$, $\vec{B}=0$, and $H_k=0$. We will also neglect direct contributions from acoustic phonons (considered by us) and from lattice polarons (considered by NP). If according to NP we further assume that

$$\vec{\Gamma}_k = 2A_1 \sum_j \vec{J}_j \equiv 2A_1 \vec{L}, \quad (\text{A8})$$

then according to Eq. (A7)

$$\tilde{P}_k(\vec{\Delta}) = \sum_{L=0}^{NJ} F(L) \delta(\Delta - 2A_1 L), \quad (\text{A9})$$

where $F(L)/(2L+1)$ is the number of ways in which N moments each equal to J can combine to give the total spin L .¹⁴ With these simplifications the hopping probability (A6) can be evaluated as

$$\begin{aligned} w_{12} &\propto \frac{\sum_{L=0}^{NJ} F^2(L) \cosh(A_1 L/T)}{\sum_{L,L'=0}^{NJ} F(L) F(L') \cosh(A_1 L'/T)} \\ &\approx \frac{\sum_{L=0}^{NJ} F^2(L) \exp(A_1 L/T)}{\sum_{L,L'=0}^{NJ} F(L) F(L') \exp(A_1 L'/T)}. \end{aligned} \quad (\text{A10})$$

This formula coincides with the NP formula (15) if in the latter the lattice polaron energy $E_a \rightarrow 0$. Moreover,

$$F(L) \approx \frac{1}{\sqrt{\pi}} \left(\frac{3}{2J(J+1)N} \right)^{3/2} (2L+1) \exp\left(-\frac{3L^2}{2J(J+1)N} \right), \quad (\text{A11})$$

which can be justified for $1 \ll L \ll JN$, i.e., when the magnetization is relatively far from saturation (see Ref. 11 for details). Substituting Eq. (A11) into Eq. (A10) and evaluating the sums by means of the steepest descent method yields

$$w_{12} \propto \exp[-W_p(0)/2T], \quad (\text{A12})$$

where $W_p(0)$ is given by Eq. (40) with $T_0=0$, i.e., with the Curie-Weiss magnetic susceptibility. This is also in clear agreement with the numerical results of NP (see NP, Fig. 1) as well as with our analytical results (see Sec. V).

APPENDIX B: PHONON-ASSISTED HOPPING

Our next step is to evaluate the phonon-assisted part $w_{12}^{(ph)}$ of the hopping rate (22) by replacing the summation over q by an integration. We will also use the standard dispersion law for acoustical phonons, $\omega_q = sq$, together with the following expression for the electron-phonon coupling matrix element:^{19,21}

$$|\Lambda_q|^2 = \frac{E_1^2}{ds^3 V_0^{1/2} \hbar q} (1 - \cos \vec{q} \cdot \vec{r}_{12}) \rho_{\vec{q}}, \quad (\text{B1})$$

where E_1 is the deformation potential, V_0 is the total volume of the system, d is its density, s is the speed of sound, and

$$\rho_{\vec{q}} = \frac{1}{\sqrt{V_0}} \int_{V_0} |\Psi|^2 e^{i\vec{q} \cdot \vec{r}} d\vec{r} \quad (\text{B2})$$

is the Fourier transform of the localized-electron density. It gives

$$\begin{aligned} w_{12}^{(ph)} &= \frac{\sqrt{\pi} |t|^2}{2\hbar T} (p_{12}^{(ph,+)} + p_{12}^{(ph,-)}) \\ &\approx w_0 \frac{E_1^2 V_0^{1/2}}{2\pi^2 ds^3 \hbar} \int_0^{q_D} dq q \rho_q \left(1 - \frac{\sin qr_{12}}{qr_{12}} \right) \\ &\quad \times \left[N_q \exp\left(-\frac{(2W_p - \epsilon_{12} - \hbar qs)^2}{8W_p T} \right) \right. \\ &\quad \left. + (N_q + 1) \exp\left(-\frac{(2W_p - \epsilon_{12} + \hbar qs)^2}{8W_p T} \right) \right], \end{aligned} \quad (\text{B3})$$

where q_D is the radius of the Debye's sphere and

$$w_0 = \frac{\sqrt{\pi} |t|^2}{2\hbar T} F(\mu, \nu; 0). \quad (\text{B4})$$

In deriving expression (B3), the integrals containing terms with $\eta_{\pm} = \Delta_0(\epsilon_{12} \pm \hbar \omega_q)/4W_p T \neq 0$ [see Eqs. (22)–(25)] were omitted. They are negligibly small compared to those retained in Eq. (B3) either due to a small factor $(\epsilon_{12}/2W_p)^2 \ll 1$ when $|\epsilon_{12}| \ll W_p$ or because the corresponding integrands reach their sharp maximums at $\hbar \omega_q \approx \pm \epsilon_{12}$ (i.e., $\eta_{\pm} \ll 1$) when $|\epsilon_{12}| \gg W_p$.

We will analyze expression (B3) in the two limiting cases of (a) large polaron shifts ($2W_p \gg |\epsilon_{12}|$), which may take place at relatively small magnetic fields, and of (b) small polaron shifts ($2W_p \ll |\epsilon_{12}|$), which may be relevant for large magnetic fields when the BMPs are almost frozen out.

(a) In this case the integrands in Eq. (B3) have sharp maxima at $\hbar q_0 s \approx T \ll W_p$. This has the consequence that the optimal hopping path goes through the point where the electronic energies at both sites are close to each other, so that the hopping event is accompanied by absorption or emission of a low-energy phonon the energy of which is close to T . Then the integral in Eq. (B5) can be evaluated by means of the steepest descent method which gives

$$w_{12}^{(ph)} = w_0 \zeta \exp\left[-\frac{(2W_p - \epsilon_{12})^2}{8W_p T} \right], \quad (\text{B5})$$

where

$$\zeta \approx \frac{E_1^2 r_{12}^2 n^{4/3}}{d s^3 \hbar} \left(\frac{T}{\Theta} \right)^4. \quad (\text{B6})$$

Here n is the concentration of atoms in the crystal and Θ is the Debye temperature. A simple evaluation shows that for $T/\Theta \approx 10^{-2}$, $E_1 \approx 1$ eV, $s \approx 5 \times 10^3$ m/s, $d \approx 5 \times 10^3$ kg/m³, $r_{12} \approx 50$ Å, and the parameter $\zeta \approx 10^{-5} - 10^{-6}$. Therefore, for this regime the contribution from the phonon-assisted transitions can be neglected compared to the resonant ones [see Eqs. (22) and (23)] even though both are characterized by the same activation energy $(2W_p - \epsilon_{12})^2/8W_p$. In making those estimates we took into account the fact that qr_{12}

$\approx (6\pi^2 n)^{1/3} r_{12} T/\Theta \ll 1$. By the same token, $q_0 a \ll 1$, where a is the localization radius of the BMP. Therefore, here we used $\rho_{q_0} \approx 1/\sqrt{V_0}$ for evaluations.

(b) In the opposite case of $2W_p \ll |\epsilon_{12}|$, the integrands in Eq. (B3) reach their sharp maxima at $\hbar q_0 s = |\epsilon_{12} - 2W_p|$. In this situation, the phonon-assisted tunneling prevails over the resonant one because it either goes without activation ($\epsilon_1 > \epsilon_2$) or, when $\epsilon_1 < \epsilon_2$, it requires an activation energy $|\epsilon_{12}|$ which is much smaller than the $(\epsilon_{12})^2/8W_p$ that is needed for a purely resonant hopping.

For the sake of certainty, suppose now that $q_0 r_{12} \gg 1$ and $W_p \ll |\epsilon_{12}|$. Then, by using Eq. (B3) with w_0 equal to the preexponential factor from Eq. (27) one can easily show that

$$w_{12} \approx w_{12}^{(ph)} = \frac{V_0^{1/2} \rho_{q_0} E_1^2 |\epsilon_1 - \epsilon_2|}{\pi d s^5 \hbar^4} \begin{cases} N_{q_0}, & \epsilon_1 < \epsilon_2 \quad (\text{phonon absorption}), \\ N_{q_0} + 1, & \epsilon_1 > \epsilon_2 \quad (\text{phonon emission}), \end{cases} \quad (\text{B7})$$

where ρ_{q_0} is given by Eq. (B2) with $q_0 = |\epsilon_{12}|/\hbar s$ and

$$N_{q_0} = \left[\exp\left(\frac{\hbar q_0 s}{T}\right) - 1 \right]^{-1} \quad (\text{B8})$$

is Planck's distribution function. Expression (B7) is nothing but the well-known Miller-Abrahams' formula^{19,21} for the phonon-assisted hopping rate.

APPENDIX C: ϵ_3 CONDUCTIVITY

Here we will evaluate the activation energy of the BMP hopping conductivity,²¹

$$\epsilon_3 = \langle \tilde{\epsilon}_{ij} \rangle = \int_{-\infty}^{\infty} d\epsilon_j n(\epsilon_j) \int_{-\infty}^{\infty} d\epsilon_i n(\epsilon_i) \tilde{\epsilon}_{ij}, \quad (\text{C1})$$

by means of a rectangular distribution function of the electron energies:

$$n(\epsilon) = \begin{cases} 1/\delta, & |\epsilon| < \delta/2, \\ 0, & |\epsilon| \geq \delta/2. \end{cases} \quad (\text{C2})$$

(We count the energies ϵ and the Fermi level E_F with respect to the middle of the "impurity" band which width is equal to δ .) After substituting $\tilde{\epsilon}_{ij}$, Eq. (30), into Eq. (C1) the integration yields formula (33), where

$$\epsilon_3^{MA} = \begin{cases} \delta/6 + |E_F|, & |E_F| > \delta/2, \\ 5\delta/12 + E_F^2/\delta, & |E_F| \leq \delta/2, \end{cases} \quad (\text{C3})$$

and

$$f(\alpha) = \begin{cases} \alpha^2(2 - \alpha/2)/3, & \alpha \leq 1, \\ 1 - 2/(3\alpha) + 1/(6\alpha^2), & \alpha > 1. \end{cases} \quad (\text{C4})$$

Here ϵ_3^{MA} is the Miller-Abrahams part of the activation energy that does not depend on magnetic field. It reaches its minimum value of $5\delta/12$ when the Fermi level lies in the middle of the band ($E_F = 0$). The function $f(\alpha)$ depends on a dimensionless polaron shift $\alpha = 2W_p/\delta$. The shape of this function depends on the distribution function $n(\epsilon)$, but in all cases $f(\alpha) \rightarrow 0$ as $\alpha \rightarrow 0$ and $f(\alpha) \rightarrow 1$ as $\alpha \rightarrow \infty$.

¹G.A. Prinz, Science **250**, 1092 (1990).

²R.K. Nesbet, IBM J. Res. Dev. **42**, 53 (1998).

³S.S.P. Parkin, N. More, and K.P. Roche, Phys. Rev. Lett. **64**, 2304 (1990).

⁴M. Julliere, Phys. Lett. **54A**, 225 (1975).

⁵J.S. Moodera, J. Nowak, and R.J.M. van de Veerdonk, Phys. Rev. Lett. **80**, 2941 (1998).

⁶T. Dietl, in *Diluted Magnetic Semiconductors*, edited by M. Jain (World Scientific, Singapore, 1991), p. 141.

⁷D.R. Schmidt, J.P. Ibbetson, D.E. Brehmer, C.J. Palmström, and S.J. Allen, in *Magnetic Ultrathin Films, Multilayers and Surfaces-1997*, edited by J. Tobin *et al.*, MRS Symposia Pro-

ceedings No. 475 (Materials Research Society, Pittsburgh, 1997), p. 251.

⁸T. Kasuya and A. Yanase, Rev. Mod. Phys. **40**, 684 (1968).

⁹E.L. Nagaev, Zh. Éksp. Teor. Phys. **54**, 228 (1968) [Sov. Phys. JETP **27**, 122 (1968)]; *Physics of Magnetic Semiconductors* (MIR Publishers, Moscow, 1972).

¹⁰T. Dietl and J. Spálek, Phys. Rev. B **28**, 1548 (1983).

¹¹P.A. Wolff, in *Semiconductors and Semimetals*, edited by R.K. Willardson and A.C. Beer (Academic Press, New York, 1988), Vol. 25, p. 413; D. Heiman, P.A. Wolff, and J. Warnock, Phys. Rev. B **27**, 4848 (1983).

¹²T. Dietl, J. Antozsewski, and L. Swierkowski, Physica B **117** & **118**, 491 (1983).

- ¹³A.S. Ioselevich, Zh. Éksp. Teor. Fiz. **43**, 148 (1986) [JETP Lett. **43**, 188 (1986)]; Phys. Rev. Lett. **71**, 1067 (1993).
- ¹⁴E.L. Nagaev and A.I. Podel'shchikov, Fiz. Tverd. Tela (Leningrad) **24**, 3033 (1982) [Sov. Phys. Solid State **24**, 1717 (1982)].
- ¹⁵T. Holstein, Ann. Phys. (N.Y.) **8**, 343 (1959); D. Emin, in *Electronic and Structural Properties of Amorphous Semiconductors*, edited by J. Mort (Academic Press, New York, 1973), p. 261; D. Emin, Phys. Rev. B **43**, 11 720 (1991).
- ¹⁶A.G. Petukhov and M. Foygel, Zh. Éksp. Teor. Fiz. **95**, 1037 (1989) [Sov. Phys. JETP **68**, 597 (1989)]; A.G. Petukhov, Fiz. Tverd. Tela (Leningrad) **32**, 168 (1990) [Sov. Phys. Solid State **32**, 94 (1990)]; M. Foygel, A.G. Petukhov, and A.S. Andreyev, Phys. Rev. B **48**, 17 018 (1993).
- ¹⁷L. D. Landau and E. M. Lifshitz, *Statistical Physics* (Pergamon Press, Cambridge, England, 1980).
- ¹⁸D. Schmidt, A.G. Petukhov, M. Foygel, J.P. Ibbetson, and S.J. Allen, Phys. Rev. Lett. **82**, 823 (1999).
- ¹⁹A. Miller and E. Abrahams, Phys. Rev. **120**, 745 (1960).
- ²⁰A.J. Leggett, S. Chakravarty, A.T. Dorsey, M.P.A. Fisher, A. Garg, and W. Zwerger, Rev. Mod. Phys. **59**, 1 (1987).
- ²¹B.I. Shklovskii and A.L. Efros, *Electronic Properties of Doped Semiconductors*, Springer Series in Solid State Sciences, Vol. 45 (Springer-Verlag, Berlin, 1984).
- ²²K. Binder and A.P. Young, Rev. Mod. Phys. **58**, 801 (1986).
- ²³J.H. Harris and A.V. Nurmikko, Phys. Rev. Lett. **51**, 1472 (1983).
- ²⁴D.D. Awschalom, J.-M. Halbout, S. von Molnar, T. Siegrist, and F. Holtzberg, Phys. Rev. Lett. **55**, 1128 (1985).
- ²⁵S.J. Allen, Jr., F. DeRosa, C.J. Palmström, and A. Zrenner, Phys. Rev. B **43**, 9599 (1990).
- ²⁶D.E. Brehmer, K. Zhang, C.J. Schwarz, S.P. Chau, and S.J. Allen, Appl. Phys. Lett. **67**, 1268 (1995).
- ²⁷A.G. Petukhov, W.R.L. Lambrecht, and B. Segall, Phys. Rev. B **53**, 3646 (1996).